

Chapter 14

Safety System

14.1 Personal Protection System

14.1.1 Overview

The interlock used in the personal protection system (PPS) is structured under the policy that The interlock system uses hard wires and does not use the network nor general purpose computer. Programmable Logic Controller (PLC) is regarded as having the same level of reliability as hard wire because its function is specialized in a single process. It plays an important role in PPS. The PLCs are installed in each local control room, and the information used for interlock is gathered as ON / OFF logic signal from the central PLC system through the optical fiber cable.

14.1.2 Access Control

Overview

The access control of the tunnel is carried out based on the following three levels. They are 1: Free, 2: Limit, 3: Keep out. " Free " is in a state that a person can enter the radiation control area without contacting the central control room. This state is occurred during a long accelerator shutdown period. " Limit " indicates a state temporarily allowing entry into the tunnel during accelerator operation period. In this case, the entrant needs the shift leader's permission, and the entry area is strictly managed by the surveillance camera, the card reader, the personal key. " Keep out " is a state that no one can enter the tunnel where the beam is injected or accumulated on the accelerator. At the boundary of each accelerator, "the boundary area" is provided as much as possible to reduce the radiation effect from the adjacent accelerator which is under operation. At the boundary area of each accelerator, the key of the door is

Control System (EPICS) framework[1]. The analog cameras are used in the tunnel, and the high quality digital cameras are used at the entrance to identify the entrant.

14.1.3 Logics of PPS

Whole system

The absence of beams in the tunnel is secured by at least two independent interlocks. The injector linac can simultaneously supply beams to five rings of PF, PF-AR, KEKB HER, KEKB LER, PDR. In case of PDR, the beam returns to the injector from PDR. While one of the accelerator is under operation, a person may access to the other accelerator tunnel, so that the logic of the injection beam request becomes complicated. The accelerator excluding PF requests the beam in the same procedure. The procedure from the “ Free ” state to “ the beam operation ” is shown in Table 14.1.

Table 14.1: The protocol of the beam request

	Action	State	Accelerator safety
1		Free	
2	Limit Button ON	Limit	
3	Patrol button ON	Limit	ON the BT unattended confirmation buttons
4	Keep out button ON	Keep out	
5	Beam Key ON	Keep out	The open permission of the ring stopper
6	The beam injection mode ON	Keep out	Wait an acceptance from Injector.
7	Linac accepts the mode	Keep out	The open permission of beam shutter in BT. The permission Turn ON Safety Magnet
8	Beam Request	Keep out	

First, the access level is set to "Limit", and the patrol in the tunnel is required. Because the beam transport line of KEKB is geometrically complicated, in order not to overlook person in tunnel, the unattended confirmation buttons are installed along the tunnel. To move into the "Keep out" level, all buttons have to be pushed at the patrol. After the patrol the access level moves into "Keep out" level, and the beam key is turned on. At this level, the open permission of the ring stopper is given. From the downstream accelerator to the upper stream injector, "the beam ON mode" request is sent and the injector Linac supposes to accept the request. At this stage, the safety system give a permission to turn on the safety magnet and open the beam shutter. Finally the beam request signal is sent to the injector linac.

KEKB Ring and beam transport

To permit the access to KEKB-BT line, two interlocks are required. One is to turn OFF the safety bending magnet installed in the 3rd beam switch yard at the end of the injector Linac. Another is to insert the beam shutter into the beam chamber to ensure safety. For the access to KEKB main ring, in addition above two interlocks, two more interlocks are required to ensure no stored beam in the ring. Two independent beam stoppers are inserted in the vacuum chambers in the main ring. Figure 14.2 shows the position of the safety magnets and the beam shutters on the positron and the electron beam line respectively. For the electron line, three horizontal bending magnets are connected in series to power supply, and four vertical bending magnets are connected in series to another power supply so that four vertical bending magnets and three horizontal bending magnets are used as the safety magnets.

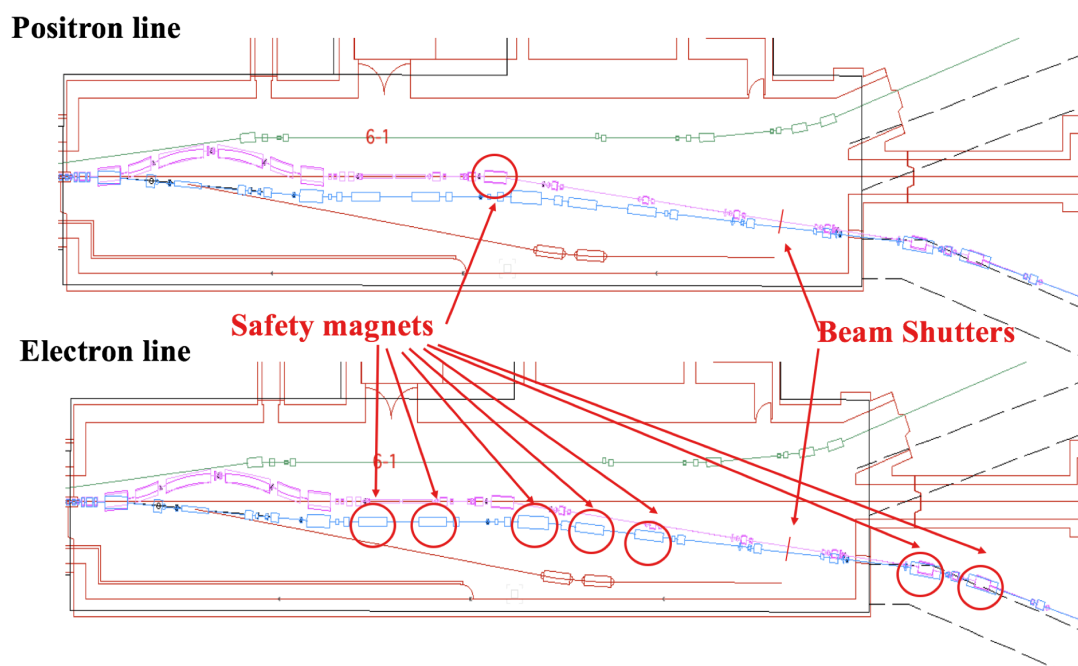


Figure 14.2: KEKB the safety magnets and the beam shutter

Damping ring

To prohibit the injection beam, one beam shutter and safety bending magnets are installed in the injection beam transport line as shown in Figure 14.3. Since the power supply drives four safety magnets which are connected in series with each other, the four magnets are used as safety magnets. No stored beam in PDR must be secured not only for PDR access, but also for the access to the injector Linac, because the

multiple accelerators. The key of the system modification to meet such demands is modularization of the system.

This system transition started with replacing the PLCs. Since the PLC of each control rooms and the central PLC system are exchanging logic signals through the optical fiber cable, the PLC system can mix a plurality of vendor models. Actually the PLC replacement has been done for several years. In addition, the access control management system is also configured independently of the main PPS and can communicate with the PPS by the logic signal, so it can be updated separately from the main PPS. The PLC system and the safety console in the central control room had to be repaired at the same time. By pre-assembling a new system, and connecting the existing cables there, the downtime is minimized. Another problem is the development and test of the PLC programing. The debugging of the PLC program with the actual accelerator is incompatible with the construction and operation of the accelerator. The programing and its verification has been done with simulation system. All input and output for example doors closed state, emergency button status, the input from console are simulated with the PLC internal relay. AT the final stage, the PLC program is verified with real accelerator.

The safety system hardware

- Whole system design:

The interlock used in the PPS is structured under the policy that it uses the hard wires and does not use the network or general purpose computer. The PLC system is regarded as having the same level of reliability as the hard wire, because its function is specialized in a single process. It becomes an important component of the system. The PLC is installed in each local control room, and the information used for interlock is gathered as ON / OFF logic signal from the central PLC system through the optical fiber cable. The information gathered through the Ethernet are used for monitor purpose, never used for the safety interlocks.

- PLC system:

To keep the low failure rate, the PLCs have been updated every ten years. For SuperKEKB PPS, Yokogawa's FA - M 3 V Leading Edge Controller is chosen. The PLCs are connected to two networks. Figure 14.4 shows the network conceptual diagram. One of the networks is connected to the sequencer CPU, and used to download the program. This network is an isolated network, it can not be accessed from outside. The other is a FA - M 3 V dedicated network called FL

- Net, which defines a common memory between PLCs and shares information. FL-Net is used only as a monitoring purpose and does not contribute to interlock. As shown in Table 2, the FL-net cluster is divided into three clusters and shares information in each cluster.

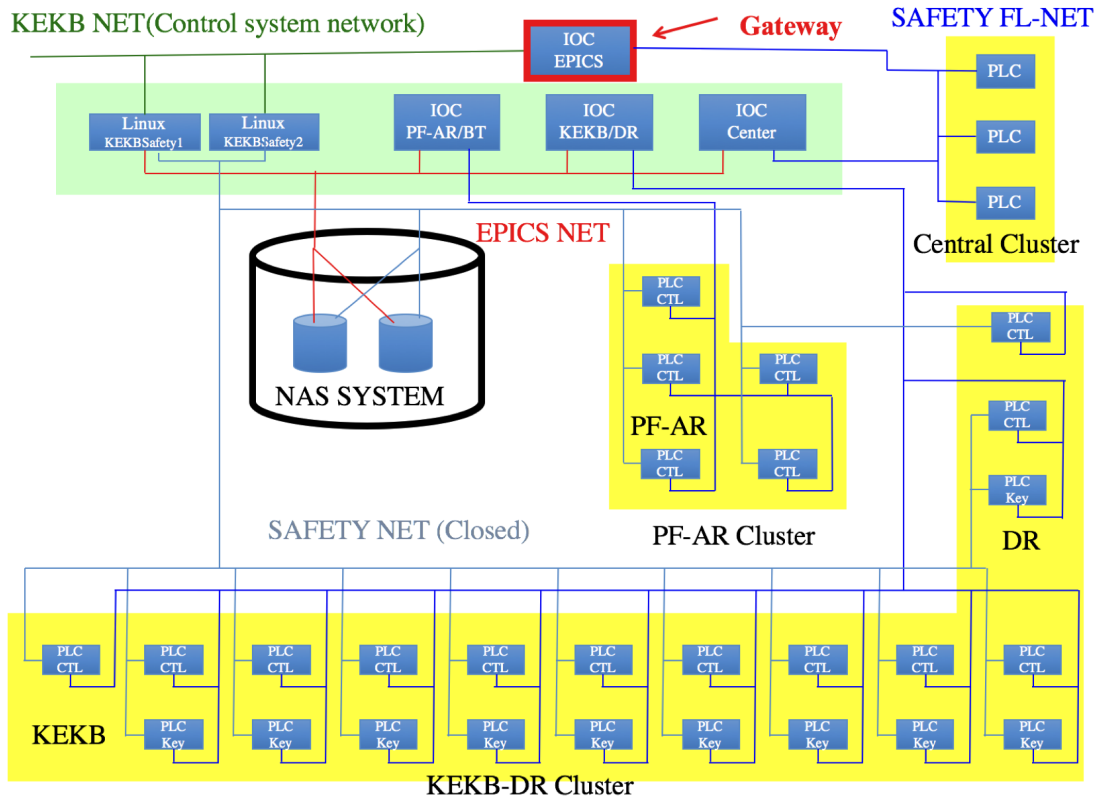


Figure 14.4: Network Configuration of PPS

- **Computing system:**
The file server and computing server are separated. As a file server, the network attached storage (NAS) has been chosen. The replica of the main file server is also installed. As a computing server, the Linux server is chosen. The Linux server connects the safety system PLC network and the network of the accelerator control system.

Software

- **EPICS based system**
EPICS is introduced to KEKB accelerator control system first, then the PPS adopts EPICS. The information obtained through the FL-net is defined as EPICS Record on the Input-Output Controller (IOC). Yokogawa's Embedded Machine

Controller (e-RT3)[2] with Linux is used as an IOC. The IOC is provided for each FL-Net cluster shown in Table 14.2. Those IOCs are connected to the Linux server computer through the third network (see Figure refsafetynet). Information of the safety system is handed over to KEKB control network through the IOC for Gateway.

Table 14.2: The FL-net Cluster

1	Accelerator Name	N of Modules	Cluster Name
2	KEKB Ring	18	KEKB Cluster
3	KEKB/BT	2	PF-AR Cluster
4	PDR	2	KEKB Cluster
5	Central	2	Central Cluster

- User interface:

All inputs that directly affect the interlock are made through the operation console. The console consists of buttons and keys, and it is connected to the input/output module of the PLCs. Since it is isolated from the network, it cannot be controlled from outside of the control room. On the other hand, the status monitor of PPS connects to the network. The open/close state of the door, the personal key return state, the state of the safety magnets and the state of the beam shutter are gathered in the IOC through FL-NET and sent to the central control room through the EPICS framework. The information is displayed using the BOY[3] of CSS (Control System Studio)[4].

- Logging system:

All the collected information is recorded and saved in the CSS archiver. Since the CSS Archiver has good affinity with EPICS, it is chosen as archiver. The information is recorded only when the value changes. Compared with polling records, it can save the logging data size as well as network bandwidth. Since the acquired data is stored using PostgreSQL which is a relational database, it can be easily displayed by a Web browser.

14.2 Machine Protection System

14.2.1 The beam abort trigger system

Overview

Figure 14.5 shows the abort trigger system configuration[5]. The abort requests from each hardware component are converted to optical signals. For the some hardware components, the 2ch E/O module (1424 module) which accepts TTL, RS422 and relay inputs, is developed. The optical signals are sent to VME-based 8 channel optical input module (18K15 module) in 12 local control rooms (LCR). The 18k15 module outputs an "OR" signal of abort requests. It also latches the signal until receiving a reset signal. These functions are processed on FPGA in the 18k15 module. The 18K15 modules collect more than 130 beam abort request signals. In the central control room(CCR), all abort requests are collected from these 18k15 module, then the abort trigger signal is sent to the abort kicker. In addition to the hardware abort trigger system, a request activated by the software is used for the abort request that do not require a quick response. The software abort requests are collected from many Input/Output Controllers (IOCs), such as IOC of RF, vacuum, monitor, etc. A manual abort was also prepared to discard the beam in the normal accelerator operation. Software abort requests and manual abort request are merged into hardware abort signals in CCR. The system is controlled in the EPICS frame work.

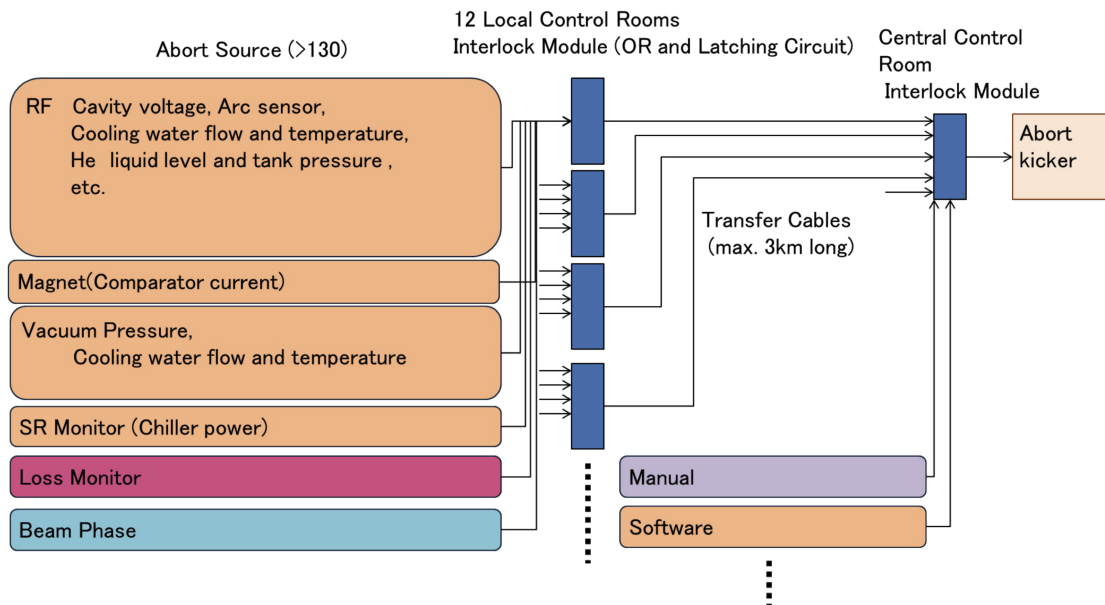


Figure 14.5: The abort trigger system at SuperKEKB

Time stamp

Since abort requests are occurred sequentially, chronological order of the request is important to identify a cause of the beam abort. The beam abort system has the time stamp function to keep track of the abort request signal. The time stamp information is recorded in the IOC located at CCR. Figure 14.6 shows timing diagram of the time stamp system. The time stamps are generated from two counters. One is the trigger pulse counter which counts as the external clock at the 18k15 module. This trigger pulse counter is used to synchronize all the 18k15 modules in the system. The external clock is relatively slow clock and it is generated by the software trigger system[6]. The software trigger system generates not only synchronization pulse for VME 18k15, but also the interrupt signal for IOCs. To get precise abort request time, the internal clock counter of 18K15 module is used. The internal clock counter count up at 10 MHz, and is synchronized to FPGA operation clock. Each counter is 32-bit counter.

Both counter values are cleared when the 18k15 module receives the reset signal. The internal clock is also cleared by the external clock input. Each counter starts after detecting the reset signal. When the abort request signal is detected in the module, both counter is latched. The common external clock determines the time roughly and the internal clock determines more precisely. The resolution of the timestamp is $0.1\mu\text{s}$ since the internal clock counter counts up at 10MHz. The time stamp value is calculated from these two counter value in the IOC. And the effect of transmission time difference, device processing delay are also corrected by the software.

Beam abort request

The beam abort system collects four types of abort requests[7].

- Triggers from beam loss monitors
- Triggers from synchrotron oscillation phase monitor
- Direct triggers from hardware components
- Manual abort signal

The circumference of SuperKEKB ring is 3km with 12 LCRs as shown in Figure 14.8 . Loss monitor signals are collected at 4 LCRs, RF signals are collected at 6 LCRs.

Response time of the beam-abort system

The time that the hardware detects the abort alarm, extends over the wide range, i.e. from a few μs to several second. For example PIN diode detect the beam loss within a

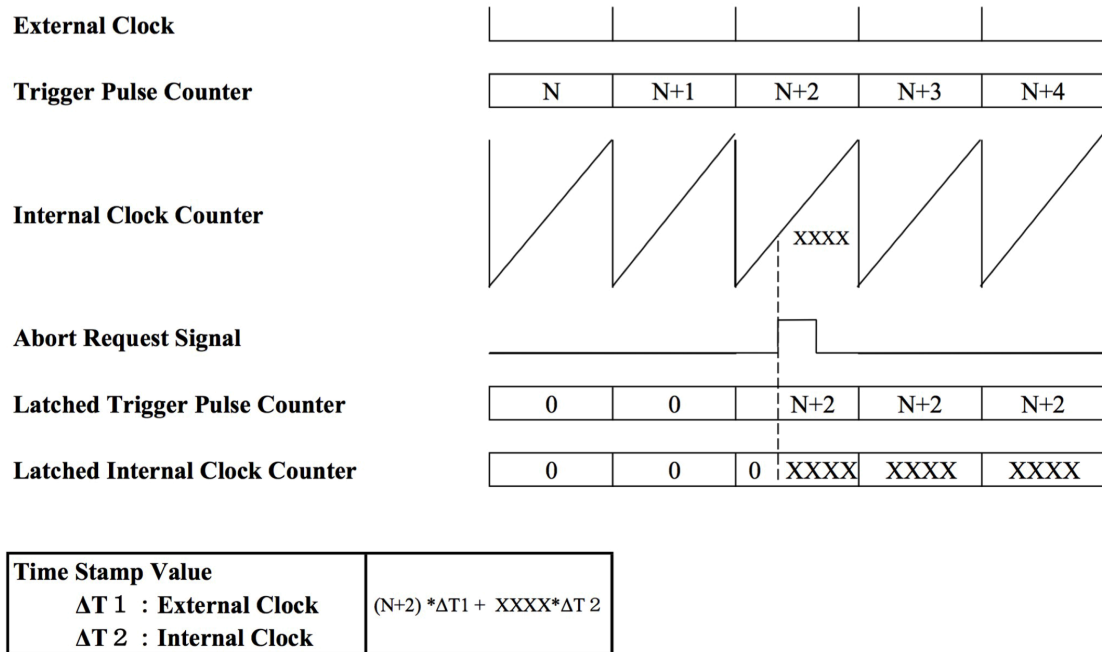


Figure 14.6: Timing chart of time stamp system.

few μs [8]. On the other hand, loss monitor of ion chamber needs several ms to generate the signal. Other device such as a magnet power supply, needs several ms to several second to detect the failure.

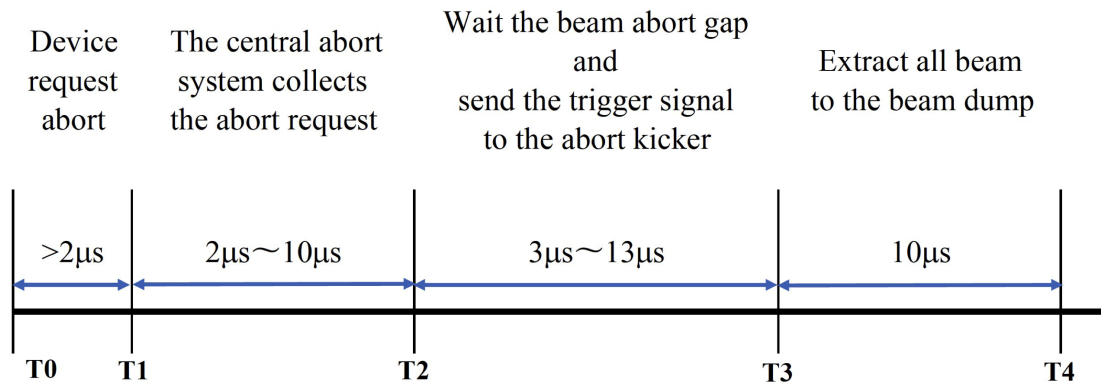
After the hardware detects the alarm status, the abort trigger system send the abort request signal to the beam abort system. The beam abort requests that require a quick response are designed to be transmitted via hardware. The time from a failure detection to the beam extraction is estimated as follows. Figure 14.7 shows the time necessary in each stage.

- T1-T0: This is the transmission time from the beam line to the interlock module at the LCR. At least $2\mu\text{s}$ is needed if the detector, such as the beam loss monitor, is located in the tunnel.
- T2-T1: The time necessary for signal processing at LCR plus transmission time from LCR to CCR. The abort signal collected at the LCR, is converted to an optical signal. This process takes 100-200ns that is negligible compared with transmission time from LCR to CCR. The longest distance from LCR to CCR is 2km, so that the maximum transmission time is about $10\mu\text{s}$. Even for the nearest LCR, $2\mu\text{s}$ is needed to transmit the signal.
- T3-T2: The revolution time of the SuperKEKB ring is $10\mu\text{s}$. The beam is filled

in every two RF buckets except for consecutive an empty bucket of 200ns that is used for rise time of the abort kicker magnet. Since abort kicker has to be fired synchronized with this abort gap, waiting time of 0-10 μ s is indispensable. Moreover it takes 3 μ s to transmit the trigger signal from CCR to abort kicker power supply as well as to turn on the kicker thyatron switch. In total 13 μ s is necessary in this stage.

- T4-T3: The time to extract all bunches from main ring by one set of abort kicker magnet.

After the device send the abort request, the beam abort system needs 17-35 μ s to extract all the beams from the ring. On the other hand the software abort response time takes few seconds.



- T0: A failure is detected
- T1: Beam abort request is sent to the central abort system from the local device
- T2: Abort kicker trigger signal is ready in the central abort system
- T3: Abort Kicker fired
- T4: All bunches are extracted

T4-T1: 17 μ s ~ 35 μ s

Figure 14.7: Overview of beam loss monitor and abort monitor system at SuperKEKB

Beam abort monitoring system

A beam abort monitor system is prepared to diagnose what caused the beam abort. The system consists of four data loggers. The data loggers are located in 4 LCRs. In each LCR, 24-32 signals are monitored. They collect various signals such as beam current measured by a DCCT; beam loss monitor signals from PIN photo-diodes (PINs) as well as ion chambers (ICs); various signals related to the RF cavities, i.e. cavity voltages

and output power of klystrons; the beam phase signal that measures the deviation from the synchronous phase; the injection trigger timing and the abort request signal. The length of logging time is between 300ms and 600ms for each abort event with a sampling time of $1\mu\text{s}$ to $5\mu\text{s}$, which depends on the type of logging apparatus. The recorded data is sent to the CCR via the KEKB control network.

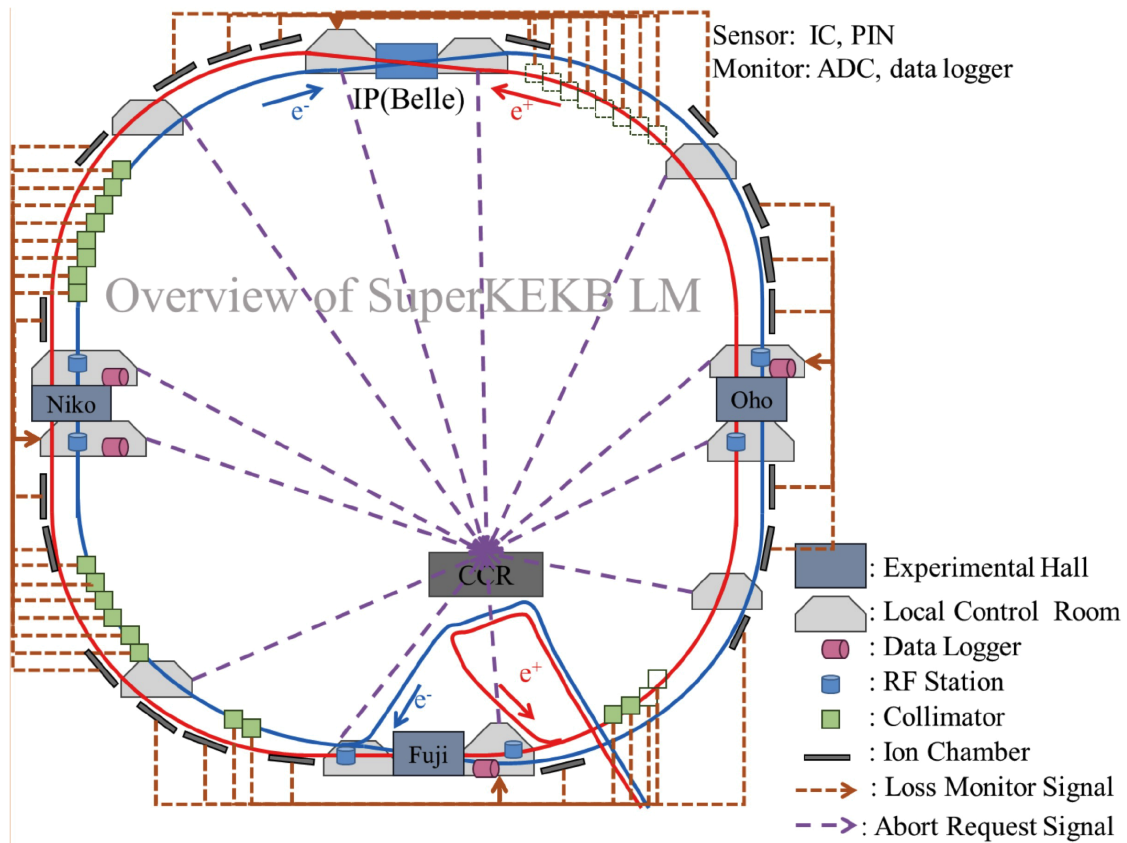


Figure 14.8: Overview of beam loss monitor and abort monitor system at SuperKEKB

14.2.2 Beam abort system

In order to protect the accelerator components and Belle II detector, each ring is equipped with a beam abort system. It extracts the stored beam and conveys to the beam dump preventing the beam spraying around the ring. Both of HER and LER abort system is installed in the Fuji straight section[9].

System requirements

Basic design There are two requirements for the beam abort system. One is to transport the extracted beam to the beam dump safely. In order to extract the beam

without damaging the extraction window made of titanium (Ti), the energy density dissipated at the Ti window is less than its allowable maximum value. The other requirement comes from the requirement for the stable operation of RF cavities. To minimize the abrupt change in beam loading, the beam abort gap that is an empty bucket space reserved for the rise time of the abort kicker magnet, must be less than 200 nsec.

The extraction window The titanium window is chosen as the extraction window, because of its small mass number and high melting point. When the beam passes through the extraction window, it deposits the minimum ionizing energy in the window. Since the thickness of the window is sufficiently thin (1.4mm), compared to the radiation length of 35.6mm, dissipated energy due to the electromagnetic shower is negligible small. Because the deposited energy due to the collision is in proportional to the thickness of the window, the temperature rise of the window is independent of its thickness. It depends on the charge density at the window. Since the beam emittance of SuperKEKB is one order of magnitude smaller than that of KEKB, the effective passage area must be enlarged to decrease the charge density at the extraction window. In the present abort system, the beam size is widened deliberately in the horizontal direction, and the effective beam cross section is expanded by sweeping the beam position in the vertical direction at the window. The energy density is determined through the product of the horizontal beam size and the sweeping height (H), as shown in Figure 14.9. Note that vertical beam size of the bunches is irrelevant.

In SuperKEKB, 2500 bunches of the beam come in every 4 ns. If the extracted beam is swept 15mm in the vertical direction, the beam spot moves $6\mu\text{m}$ per bunch. In KEKB, the maximum current was 2 A in LER and the effective charge density of extracted beam at the window is 0.3 A/mm^2 . In the new abort system, the charge density is designed not to exceed this value. In addition, the destruction limit of titanium window due to the single passage of the beam was investigated using the beam of KEKB[10], it was no damage at 0.53 A/mm^2 , while it was destroyed at 0.77 A/mm^2 . Although the effect of multiple passage (effect of fatigue or recrystallization) is still unknown, experience of KEKB tells that the density of 0.3 A/mm^2 is safe and has some margin with respect to the single passage limit of 0.53 A/mm^2 . One may concern difference of sweeping pattern at the window affects the maximum stress: in the KEKB it was sinusoidal while simple vertical sweep in the SuperKEKB. In the former case, the current density maximizes at several stationary points, while in the latter maximum points lies on the vertical line. Dynamic stress may differ between these cases. Analysis shows, however that for the Gaussian beam, maximum dynamic

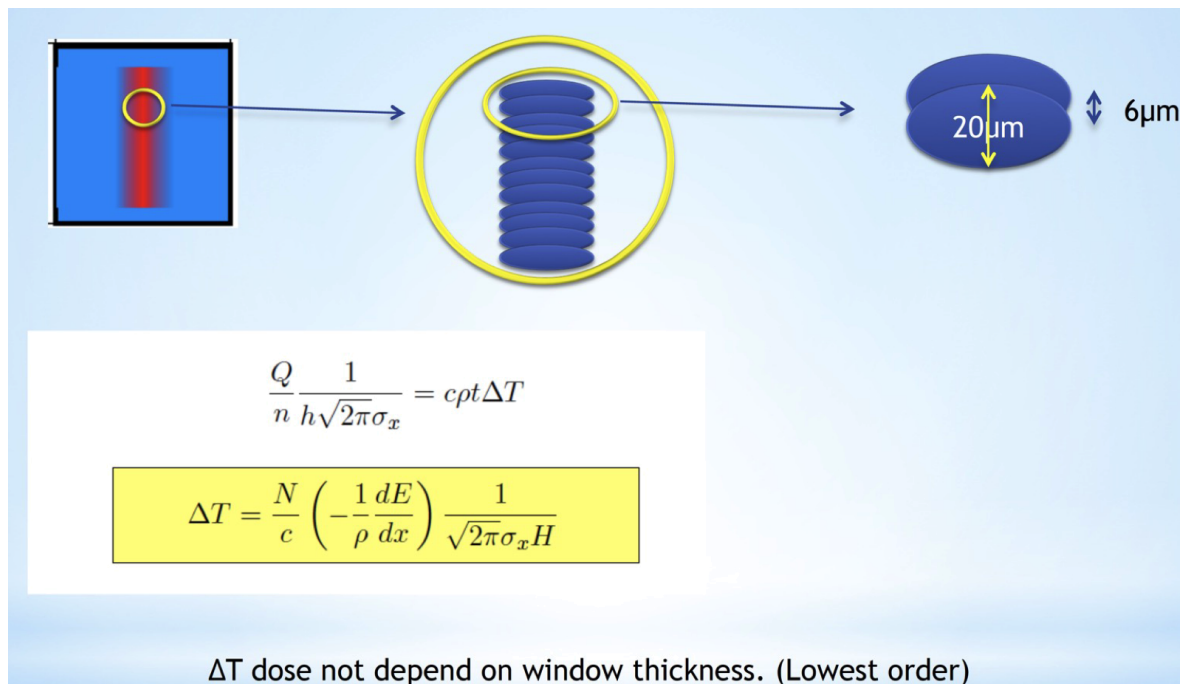


Figure 14.9: Beam profile at the extraction window

stress does not exceed its initial thermal stress; because speed of sound in the window material ($\sim 5000\text{m/s}$) is much larger than the sweep speed (2120 m/s), the dynamic stress does not accumulate; so there is no big difference in the maximum dynamic stress between both case[16]. Table 14.3 shows the beam parameters at the extraction window. Current density is 0.25 and 0.2 A/mm^2 for LER and HER, thus having margin of 20% to that of KEKB. Temperature rise is estimated to be 360°C and 290°C in LER and HER. It should be noted that the tensile strength at 400°C is as small as $1/5$ compared to that at 20°C .

Table 14.3: The beam profile at the extraction window

	KEKB(LER)	SKEKB(LER)	SKEKB(HER)
E [GeV]	3.5	4	7
ε_x [nm]	24	3.2	4.6
σ_x at abort window [mm]	0.68	1.22	1.1
Vertical Sweep ΔY [mm]	10-15	12-15	12-15
I [A]	2	3.6	2.6
I/ σ_x / ΔY [A/mm ²]	0.3	0.2-0.25	0.16-0.2

Beam-abort system of HER

Overview The schematic layout of the HER abort system is shown in Figure 14.10. The HER beam abort system consists of four horizontal kicker magnets, a vertical kicker magnet, a DC sextupole magnet, a Lambertson septum magnet, a Ti extraction window and a beam dump. The horizontal kicker magnets extract the beam from vacuum chamber through the Ti window. The abort system makes the horizontal beam size larger by the large horizontal beta function using the sextupole magnet. The vertical kicker sweeps the beam in the window during one revolution time. In order to enlarge the horizontal beam size, the DC sextupole magnet is installed between horizontal kicker magnets and the extraction window. Deflected by the horizontal kickers, the beam which passes through the sextupole off-center, is enlarged in the horizontal size due to the quadrupole component of the off-centered sextupole. The extracted beam is transported by the Lambertson septum magnet to the beam dump. Since the DC sextupole magnet degrades the dynamic aperture of the stored beam, another sextupole magnet which is connected by $-I$ or I transformation is installed to cancel the geometric aberrations.

Table 14.4: Optics parameters of aborted beams. SI and BI mean synchrotron injection and betatron injection, respectively.

	HER (SI)	HER (BI)	LER (BI)
$\varepsilon_x/\varepsilon_y$ [nm/pm]	4.6/11.5	4.6/11.5	3.2/8.6
ΔX at abort window [mm]	38	40	36.8
Vertical sweep at abort window [mm]	15	15	15
σ_x at abort window [mm]	1.2	1.1	1.22
ΔY at entrance of dump [mm]	-217	-217	-129
K0/magnet of H. Kicker (\times number) [mrad]	0.338 ($\times 8$)	0.332 ($\times 8$)	0.66 ($\times 2$)
K0 of V. Kicker [mrad]	1.28	1.31	1.99
K0 of Lambertson septum [mrad]	79.3	79.2	121.1
K2 of DC sextupole [$/m^2$]	-4.29	-4.36	—
K1/magnet of pulsed quadrupole (\times number) [$/m$]	—	—	-0.036 ($\times 2$)

Optics design Two kinds of injection scheme are planned in HER[11]. One is the betatron injection (BI) and the other is the off-momentum synchrotron injection scheme (SI). The beam abort system is designed to match the both injection scheme[12]. Figure 14.11-(a) and (b) show the optics of the betatron injection scheme for the stored

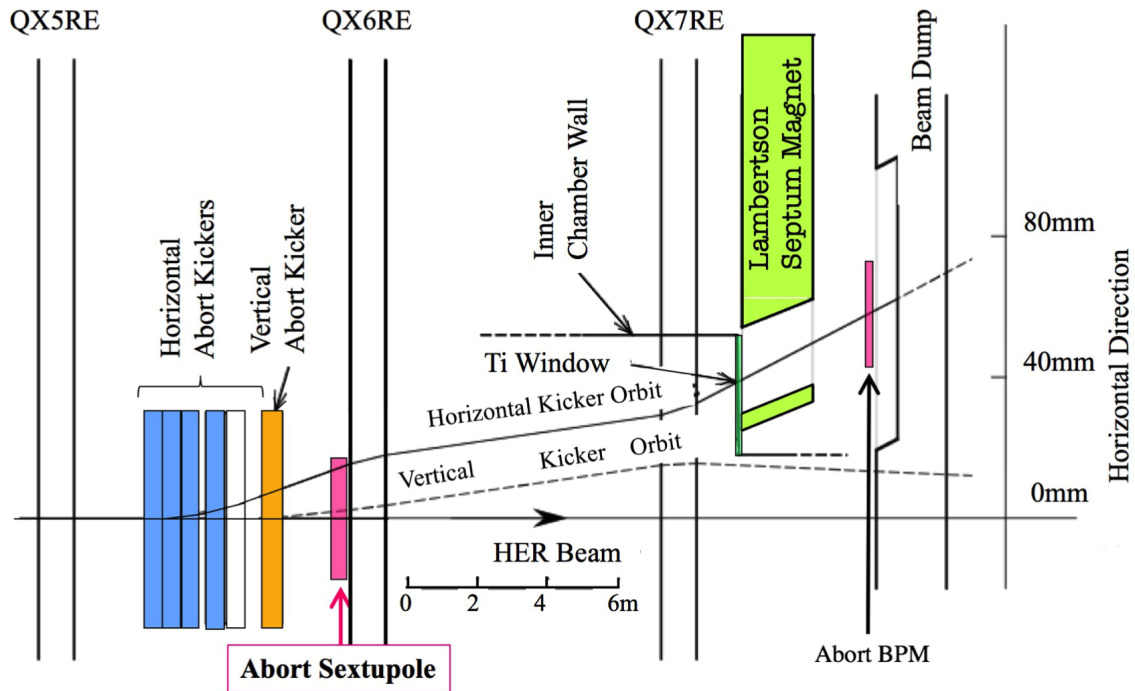


Figure 14.10: The schematic layout of the HER abort system. The horizontal axis shows the position along the electron beam. The transverse orbits at abort system region are shown. The stored beam passes the center of the abort sextupole. On the other hand, the aborted beam passes off-center of the sextupole magnet.

beam and the aborted beam, respectively. The horizontal displacement of the aborted beam is 40 mm at the extraction window. Using the sextupole magnet, the horizontal beam size is enlarged from 0.1mm to 1.1 mm at the window. The optics parameters for the abort system are summarized in Table 14.4.

As shown in Figure 14.11-a, the phase advance between the two sextupole magnets is 1.5π in the horizontal and π in vertical plane respectively. There is no dispersion at the sextupole magnet. Figures 14.12-(a) and (b) show the optics for the off-energy synchrotron injection scheme of the stored beam and the aborted beam. Since there is a horizontal dispersion in the abort section, optics was adjusted to make a dispersion function zero at the center of the abort sextupole magnet for the stored beam optics, while the slope of the dispersion was left free.

Dynamic aperture of HER The influence of the sextupole pair to the dynamic aperture is estimated. Figure 14.13 shows the dynamic apertures in the HER, where

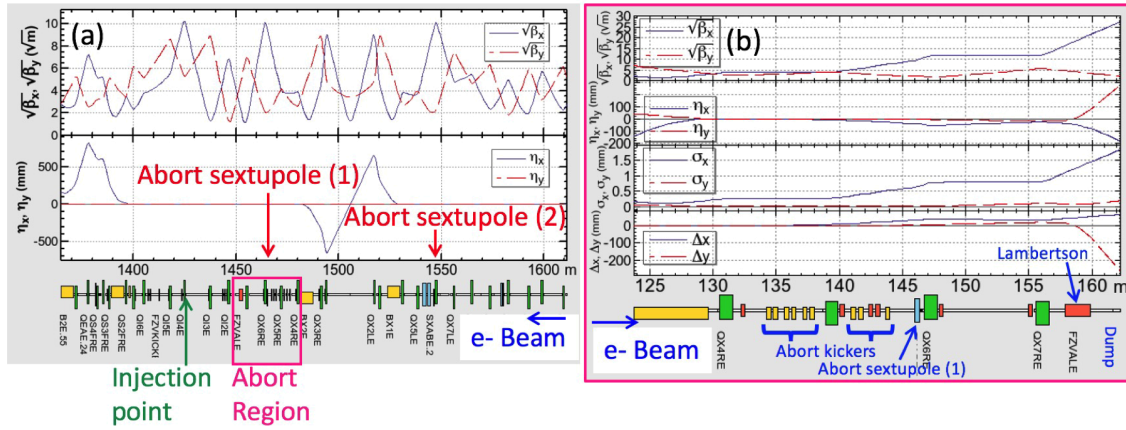


Figure 14.11: Optics of the betatron injection scheme for HER. The black and red lines correspond to the horizontal and vertical planes, respectively. (a) The beta functions, dispersion functions for the stored beam around the abort system region of the HER. The beam comes from the *right* side. (b) Zoom of (a) around the abort system for the abort beam. The beam comes from the *left* side.

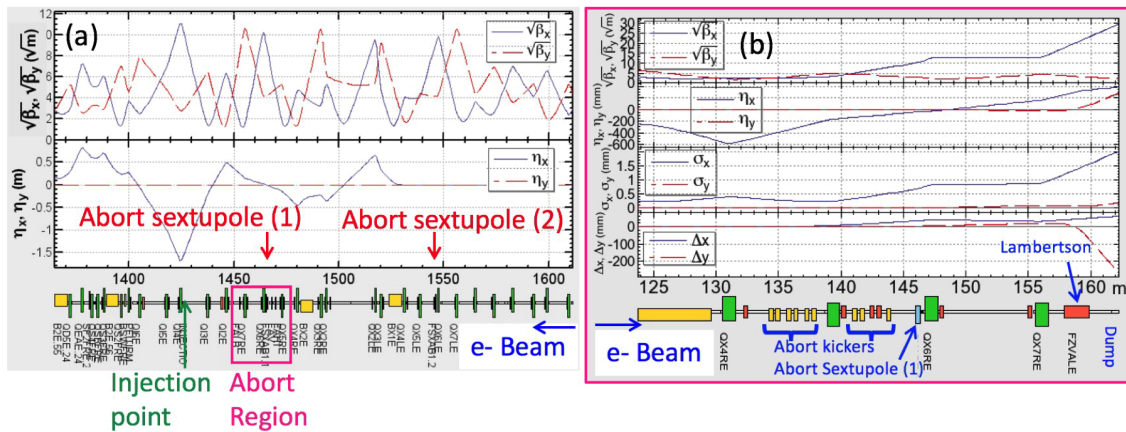


Figure 14.12: Optics for the synchrotron injection scheme in HER. The black and red lines correspond to the horizontal and vertical planes, respectively. (a) The beta functions, dispersion functions for the stored beam around the abort system region of the HER. The beam comes from the *right* side. (b) Zoom of (a) around the abort system for the abort beam. The beam comes from the *left* side.

the beta functions at the interaction point assumed to be the design value of $\beta_{x,y} = \{25, 0.30\}$ mm. The dynamic aperture is optimized using another sextupole. As the Touschek beam lifetime is insensitive to the sextupole strength K_2 , there is no adverse effect of the abort sextupoles on the dynamic aperture.

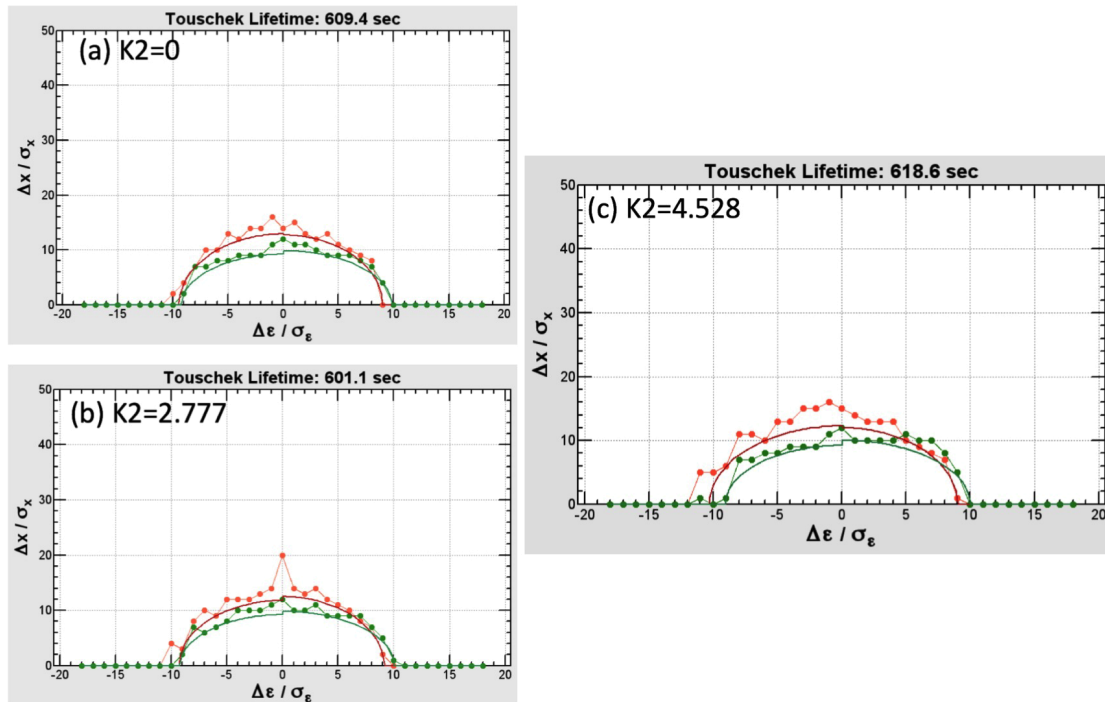


Figure 14.13: The dynamic aperture of HER for the on-energy injection scheme is shown. Red dots indicates $(\phi_{x0}, \phi_{y0})=(0,0)$ for the initial betatron phases and green dots for $(\phi_{x0}, \phi_{y0})=(\pi/2, \pi/2)$. The $K2$ values of the abort sextupole pair are, (a) zero, (b) 2.78 m^{-2} (half of the design value) and (c) 4.53 m^{-2} (design value). The Touschek beam lifetimes are estimated using smaller aperture data as (a) 610 s, (b) 600 s, and (c) 620 s, respectively.

Beam-abort system of LER

The design of abort system for the LER is almost same as that of HER. Instead of a DC sextupole magnet, two pulsed quadrupole magnets are used to enlarge the horizontal beam size. Because of geometrical reason, it was impossible to enlarge horizontal beam size by the sextupole magnet with reasonable parameters. Actually magnification of the beam size at the window by the pulsed quads is not sufficient. Fortunately horizontal dispersion function at the window helps in large fraction.

Figures 14.15-(a) and (b) show the optics for the stored beam and the aborted beam respectively. The kickers and the pulsed quadrupole magnets are located across the injection point. One horizontal kicker magnet, a vertical kicker magnet, two pulsed quadrupole magnets are used. The extraction window placed in front of the Lambertson septum, is located in the dispersion suppressor area at the end of the Fuji straight section. Besides the beta function modified by the pulsed quads, the non zero dispersion

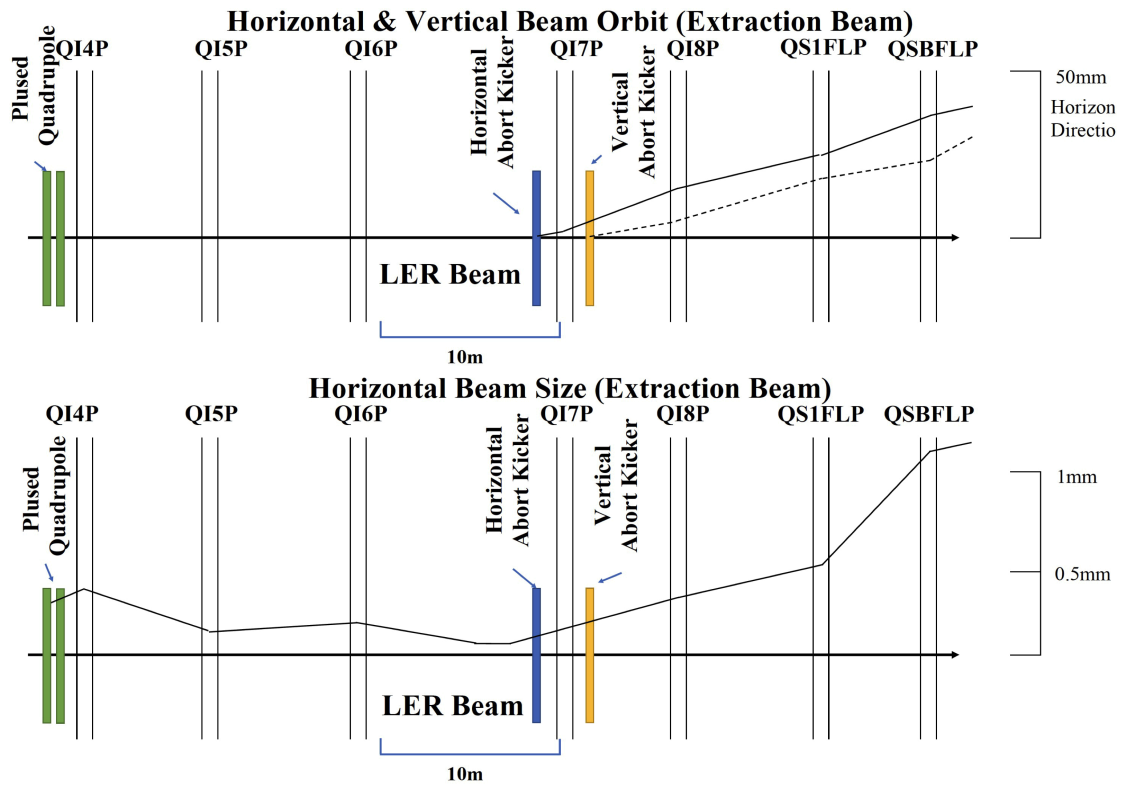


Figure 14.14: Configuration of the LER abort system.. The horizontal axis is the distance along the positron beam. The transverse orbits at abort region are shown.

at the window, contributes to make the horizontal beam size from 0.52 mm to 1.22 mm at the window . The parameters of the LER abort system are shown in Table 14.4.

System components Design

Since the most difficult part of the system is the power supply, it was designed with careful consideration. Other components are developed in harmony with the power supply design. For easy maintenance, the maximum supply voltage is designed to be less than 40 kV which makes the thyatron switch operable in the air. Horizontal physical aperture was determined by the optics requirement, and physical aperture of vertical direction was determined to match the kicker power supply. Under this condition, the kicker magnet current is set around 1.7 kA. In addition, a local heating of the surface of the ceramic chamber due to wall current of the high current beam is considered to determine the vertical aperture.

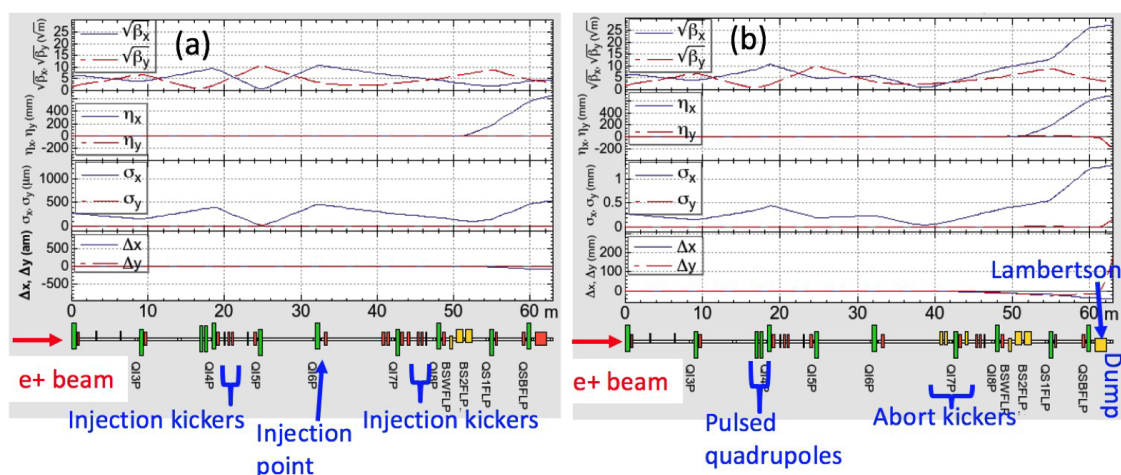


Figure 14.15: Optics of the LER abort system. The black and red lines correspond to the horizontal and vertical plane, respectively. (a) The beta functions, dispersion functions, beam sizes, and orbits for the stored beam in the abort region of the LER. The beam comes from the *left* side. (b) The same parameters as (a) for the aborted beam.

Kicker Magnets and Pulsed Quadrupole Magnets

The kicker magnets are conventional window frame magnets made of ferrite core. Table 14.5 shows the parameter of kicker magnet. The coil of horizontal kicker magnet excites the magnetic field in the two pieces of 350mm long ferrite core. Water cooled ceramic chambers are inserted into the gap.

Table 14.5: Parameters of kicker and pulsed quadrupole magnets

	HER-H	HER-V	LER-H	LER-V	LER-Quad
B or B'	23(mT)	87(mT)	25(mT)	75(mT)	1.4(T/m)
BL or B'L	63(mTm)	30(mTm)	18(mTm)	26	0.96(T)
No. of Turns (coil)	1	3	1	3	1
Core Length (mm)	350 x 8	350	350 x 2	350	350 x 2
Gap (mm)	70	90	70	90	70 (Bore radius)
No. of coils	4	1	1	1	2

As the ferrite material, PE 14 (TDK) was used. Its relative permeability is bigger than 200 up to around 10 MHz, which is sufficient for our use. Further, PE14 can be used up to magnetic field of 3 kGauss . The HER abort kicker located beside the ARES cavity. To access to the ARES cavity easily for maintenance, the kicker magnets have to be constructed as compact as possible. As shown Figure 14.16(B),

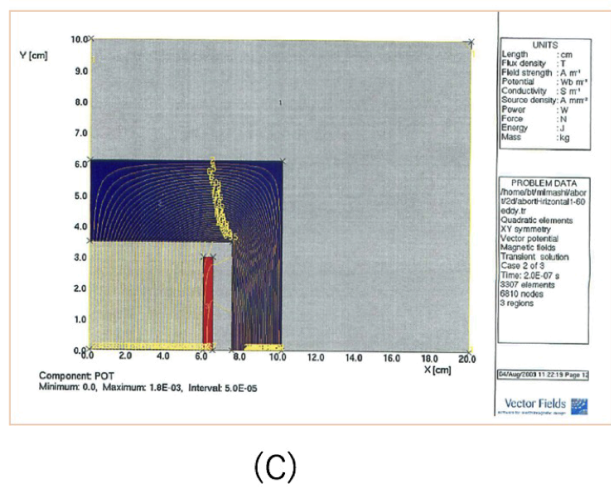
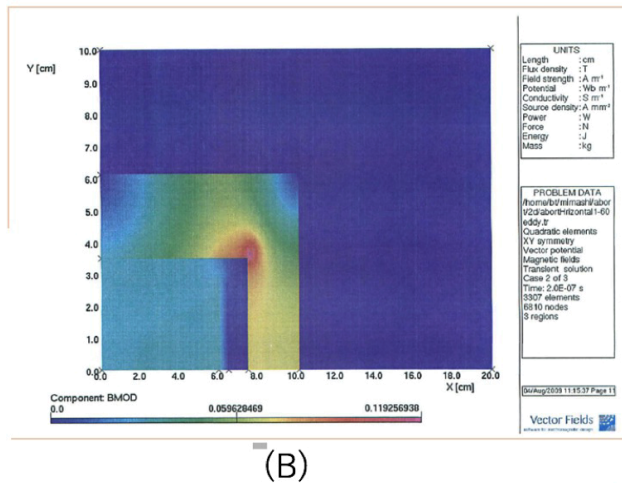
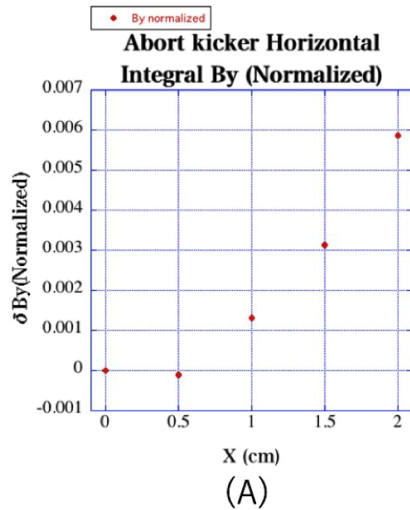


Figure 14.16: Horizontal kicker magnetic field simulation

the return yoke is made as thinner as possible under the condition that the ferrite is not saturated. To minimize the inductance, the single turn coil is chosen for the horizontal kicker and the pulsed quad. On the other hand, the vertical kicker coil has three turns. The coil of the quadrupole magnet is molded in one piece. In order to insert the ceramic chamber into the coil, one of flange is made removable. Flux line of horizontal kicker magnet is shown in Figure 14.16(C). The magnetic field uniformity is shown as a function of horizontal position in Figure 14.16(A). To improve the field uniformity, the height of the electrode in the core is designed as wide as possible to prevent the horizontal field component penetrating into the beam area. Figure 14.17 shows the configuration of HER kickers in the tunnel. The saturable inductor circuit is placed beneath the magnets. In order to protect semiconductors used in the circuit from radiation damage, the coil electrode is extended vertically and connected to the circuit at 500 mm below the beam line. Semiconductors are placed at further 200 mm lower in the tank. Two parallel wide copper-electrode were molded together in a coil.

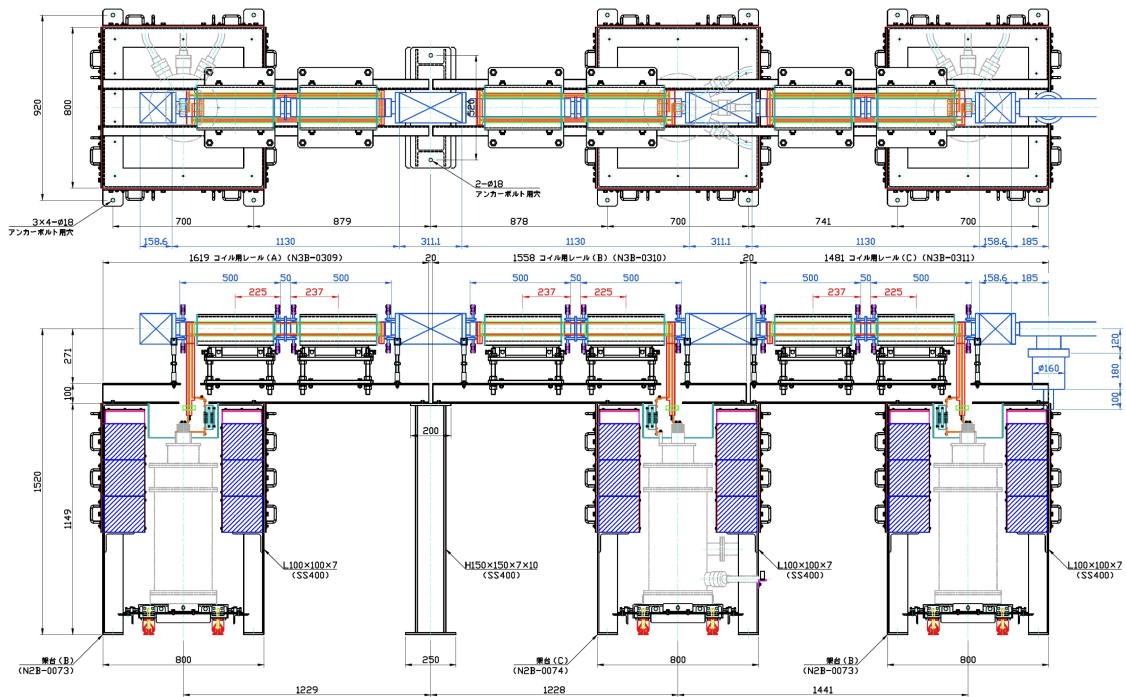


Figure 14.17: HER kicker magnet configuration at the beam line.

It minimizes the coil inductance. In order to prevent from traveling discharge on the coil surface, unevenness was introduced on the mold surface to make discharge path longer.

Power supplies

Power supply design There are two requirements for the power supply. One is a very fast rise time that is less than 200 nsec. The other is to keep current constant in time longer than one revolution time. In order to obtain a fast rise time, a saturable inductor switch was adopted and in order to feed the constant current, a power crowbar circuit was combined. Figure 14.18 shows a conceptual circuit diagram. During the first 200 nsec, the current flows through the saturable inductor circuit. At the beginning, the inductance is high and the current virtually does not flow until the integrated current exceeds a threshold where the core of transformer saturate, thereby the inductance decreases abruptly and the current starts to flow rapidly. Because the change of inductance is based on the characteristic of the core material, the switching speed is so high that rise time is determined only by the external circuit. On the other hand, the current of power crowbar circuit rises slowly. It reaches its maximum value when the current of the saturable inductor becomes zero, and keeps the current more than $10\mu\text{sec}$. Figure 14.19 shows output current of the power supply, illustrating the

transition of the two circuits. The current waveform of the vertical kicker is half sine with its maximum at about 15μ sec, which makes the vertical beam position at the window move uniformly during one revolution time. The charger and thyatron housing are located at the klystron gallery on the ground. The main capacitor, saturable inductor and power crowbar diodes are placed underneath the magnet. Since same voltage of the common high voltage power supply is applied to each horizontal and vertical kicker's main capacitor, relative strength between them can be adjusted by adding the extra resistor series to the vertical kicker magnet. The applied voltage to

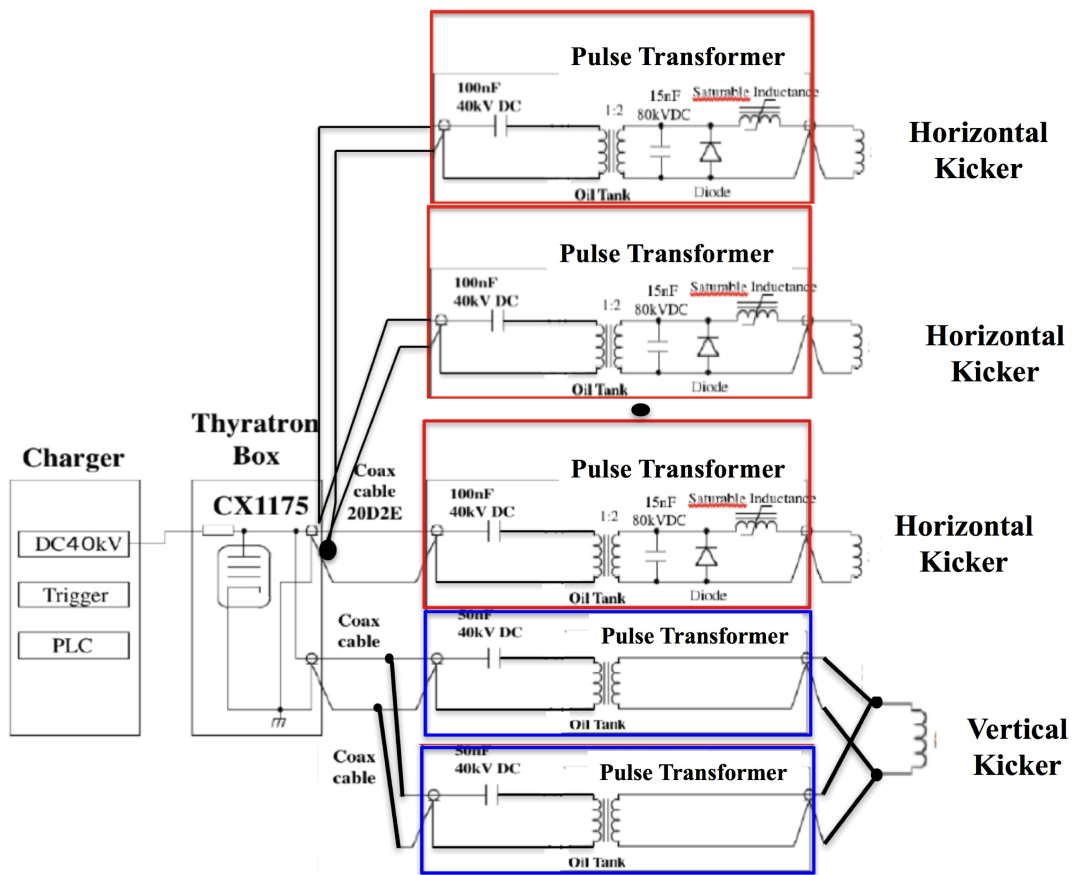


Figure 14.18: Power supply configuration. (HER)

the switching thyatron is at most 40 kV, so that it can be operated in the air. However at the main capacitance and the saturable inductor circuit, the voltage becomes about twice of the voltage at the thyatron, and they are housed in insulating oil tank placed beneath the magnet. Since it is undesirable to stock inflammable material inside the tunnel, silicone oil was used as insulating oil. Furthermore, the conservator is designed to be closed system. The thermal expansion of silicone oil is absorbed by attaching a bellows to the conservator. In order to facilitate access to the surrounding equipment,

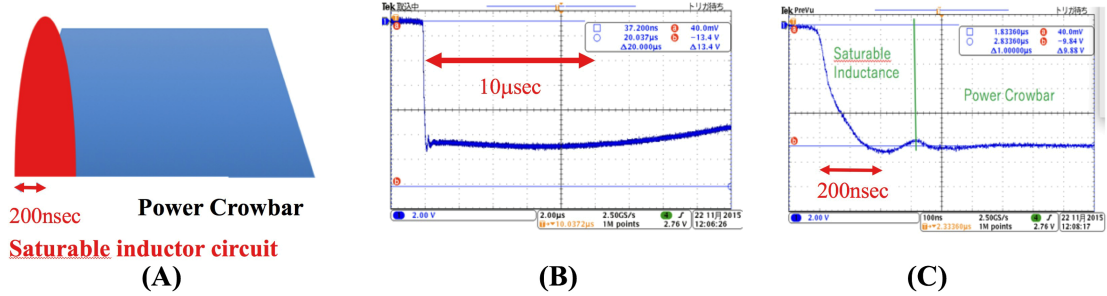


Figure 14.19: Output current in the horizontal kicker power supply. (A) Current component diagram Red part is the current from saturable inductance circuit and blue is the current from power crober circuit. (B) Output current f the horizontal kicker power supply. (C) First $1\mu\text{sec}$ of (B).

the conservator is placed just above the magnet. In designing the power supply, one of the important concept is modularization. If the power supply breaks down, it must be recovered promptly. Especially high voltages handling parts must be modularized for quick replacement with spare module in case of failure. Since the main capacitance and the saturable inductor are implemented in an oil tank, it is modularized and can be replaced easily. In addition, the parameters of the kicker magnet system are chosen the spare parts to be shared in HER and LER. In order to reduce the noise from kicker system, the ground is separated from other DC magnets. The thyatron unit and the main capacitor are connected with a double-shield coaxial cable, and the outer shield is connected to the ground on one end. Trigger signal and control network are sent through optical fibers.

Damage of accelerator components caused by the power supply failure

Damage of the accelerator components caused by the failure of the abort kicker power supply is investigated and the results is summarized in Table 14.6. All magnets are operated by a common switching thyatron to prevent either kicker magnet from improper firing. When the thyatron has a trouble, none of them are fired, and the abort does not occur. In this case the beam is sprayed in the whole ring by switching off the RF cavities or by turning off one of the weak bend magnets. It is ignited by the interlock system to prevent the damage of the vacuum chamber.

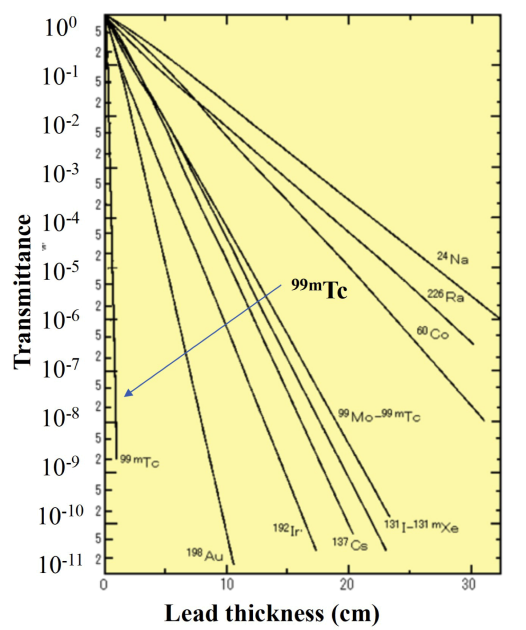
If the vertical kicker does not sweep because of the capacitor breakdown, the beam would hit a single point at the extraction window inducing a horrible damage. To avoid the damage, the main capacitance and the transformer of the vertical kicker circuit are divided into two identical parts, and connected to the kicker coil in parallel. The dual circuit system makes it possible to perform the vertical sweep even if either capacitance

Table 14.6: Abort system failure possibility

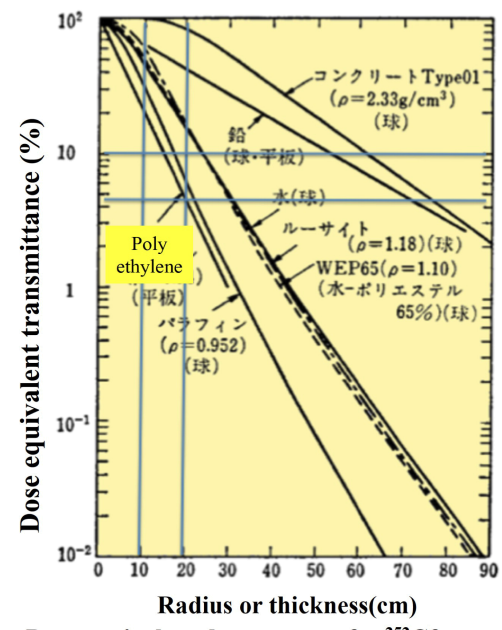
Failure events	What happen in the system	Damage
Thyratron break down	2% improper beam loss	No
Gate circuit malfunction	2% improper beam loss	No
Thyratron misfire	Off one bending magnet	No
Gate circuit misfire	Off one bending magnet	No
H-kicker cap break down (charging)	Off one bending magnet	No
V-kicker cap break down (charging)	Off one bending magnet	No
Charger fault	Off one bending magnet	No
H-kicker bias circuit fault	Off one bending magnet	No
H-kicker power crober fault	Off one bending magnet	No
V-kicker cap break down (discharge)	Small vertical sweep	No
H-kicker cap break down (discharge)	Peak current low	Damage ?

is short-circuited. The damage caused by the horizontal kicker trouble is investigated. In the case of LER, because there is only one horizontal kicker, the beam is not kicked out, and the beam is lost while sweeping in the vertical direction. The beam does not hit stationaly any single point of the vacuum chamber. In the case of HER, even if one of the kicker magnet circuit fails, except for the one at the most upstream, still the beam passes through the Ti extraction window. If the kicker magnet on the most upstream side of HER fails, there is a possibility giving the damage to the junction point of Ti window chamber and nearby vacuum chamber. To cover this case, strength of the most upstream kicker is adjusted to be weaker than other kickers.

Radiation protection The nuclear reaction that generates neutrons in SuperKEKB is mainly photo-nuclear reaction. It is close to fission neutron at Eth: 10-19 MeV (light), 4-6 MeV (Heavy). When considering shielding from the neutron in above energy range, the reference can be made to the neutron data of the spontaneous fission source of ^{252}Cf . The average neutron energy of ^{252}Cf is about 2 MeV. As shown in Figure 14.20, the neutron flux can be reduced to 1/20 with 20 cm of polyethylene. About the γ ray shield, the critical energy in SuperKEKB is about 5-10 KeV. The γ ray from $^{99\text{m}}\text{Tc}$ is 142.7 keV which is shown in Figure 14.20. So it is better shielded than $^{99\text{m}}\text{Tc}$. The sandwich of lead plate and polyethylene (lead 7 mm + polyethylene 20 cm + lead 1 mm) makes that γ ray to be on the order of 10^{-6} and neutron rays to be 1/20. γ ray generated by neutron in polyethylene shield is stopped with 1mm lead plate.



Transmittance of gamma rays in lead.



Dose equivalent decay curves for ²⁵²Cf neutrons in various spherical and flat shields.

[Source]Japan Isotope Association: The isotopes Hand Book (3rd edition) Maruzen (April 1995) p.426

Figure 14.20: Radiation shielding effect [13].

Monitor for the beam abort system

Three kinds of beam abort monitoring system is prepared.

- A screen monitor is installed in front of the beam dump. It is used usually at start-up of the accelerator operation after long shut-down. The abort kicker trigger timing is adjusted with the screen monitor.
- The output current of the kicker power supply is observed with an oscilloscope together with abort trigger signal. The monitoring plays a role as watch-dog of the abort kicker power supply.
- A beam position monitor is installed in front of the beam dump[14]. The signal from the BPM is sent to the oscilloscope, and the position of each bunch is measured. Even the abort kicker works properly, the beam loss may occur in the ring before the beam abort. The abort BPM logs the situation of extracted beam all the time, and see if the storage beam is extracted properly to the beam dump. The Figure 14.21 shows the typical aborted position of the bunches at the KEKB abort BPM. If the plots are almost same as the reference, the beam has been extracted safely.

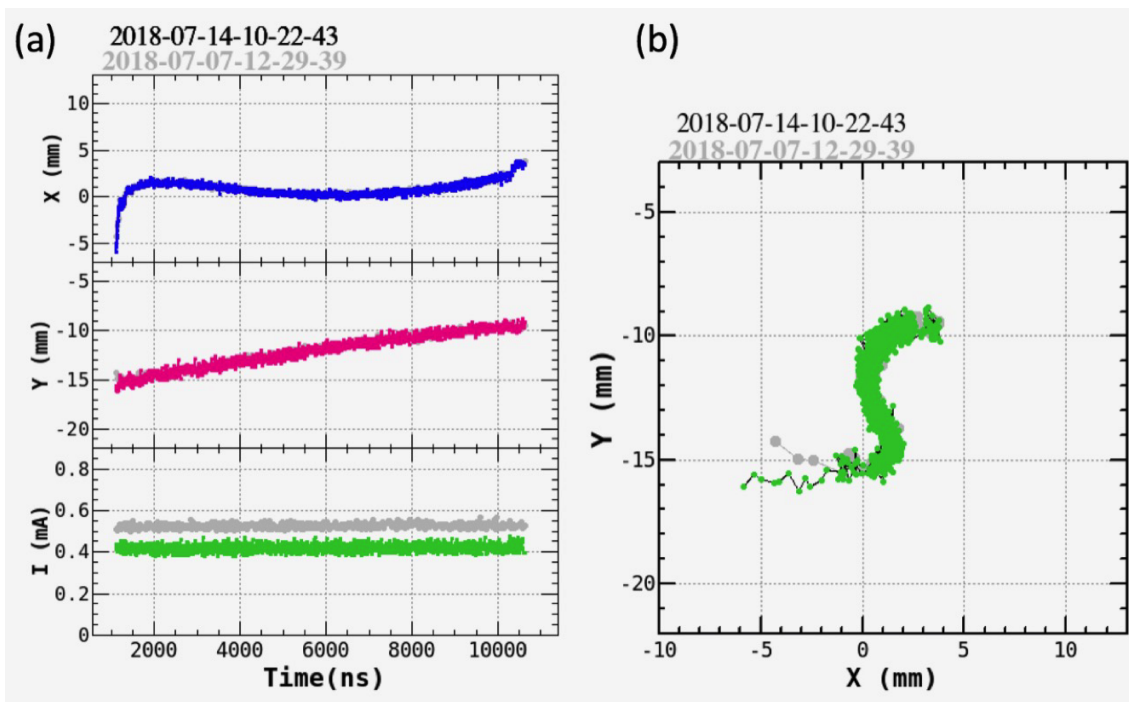


Figure 14.21: (a) The horizontal axis shows the time from the abort trigger. The vertical axes show the horizontal/vertical bunch position, and the bunch current. (b) Two-dimensional position plots are shown. The origin is the center of the BPM chamber. The gray points show the reference plots aborted manually.

Ceramic chamber

Ceramic chambers are used for the pulsed magnets in the abort system.

They enable time-varying external magnetic-field to penetrate the vacuum chamber. A thin metallic coating is necessary to carry the beam image current and also to protect outside components from the beam field. The power loss in the ceramic tube is produced by two types of induced currents. One is the image currents of the beam and the other is the eddy currents induced by the kicker's magnetic field. In case of ceramic chambers used in SuperKEKB, the power dissipation due to the beam image current is dominant. Since the design bunch length is almost same as that of KEKB, the power dissipation at the ceramic chambers can be estimated using the data in KEKB operation. The power dissipation is proportional to the number of bunches and the bunch current squared. For the SuperKEKB design current (HER 2.6A and LER 3.6A), the power loss of one ceramic tube is estimated to be 2.7kW in LER and 1.8kW in HER. Thus the water-cooled ceramic chambers are inevitable. Assuming water flow rate of 3 ℓ /min, the temperature rise of the ceramic tube is estimated to be 8°C in HER, and 14°C in LER. An independent cooling water system for the ceramic chamber

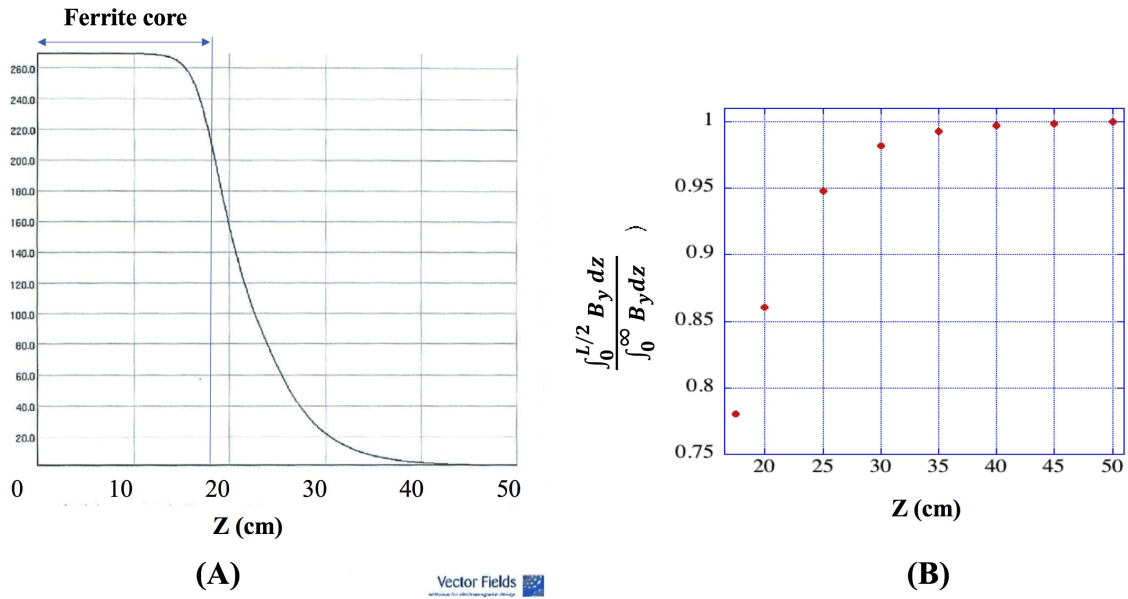
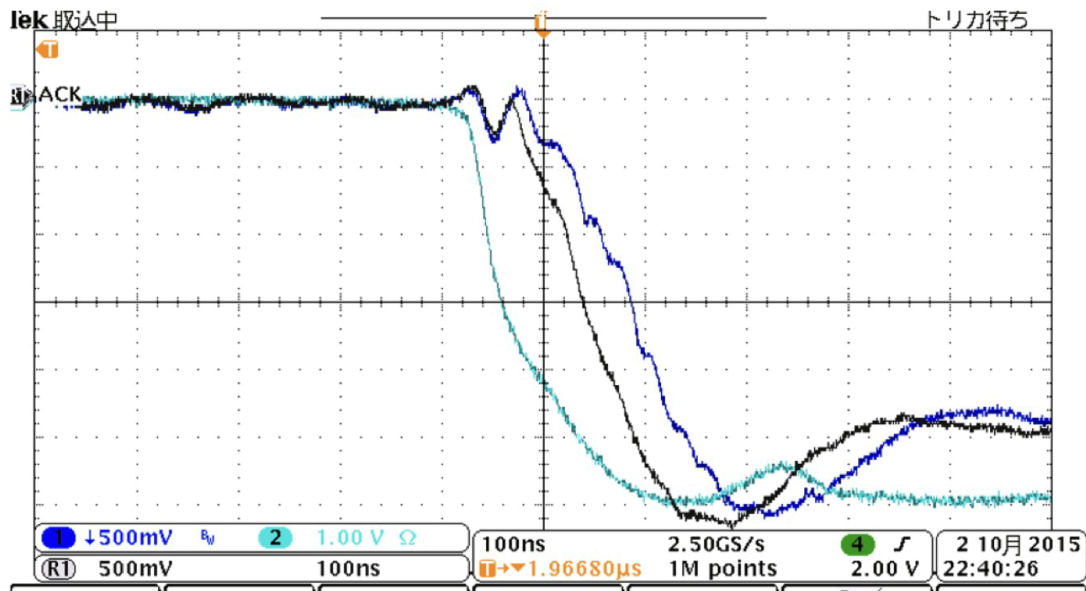


Figure 14.22: (A) Simulation result of the field distribution of the horizontal kicker along the beam. (B) Ratio of the integrated field to the total integrated field in whole region as function of z .

to the facility cooling water system directory is adopted, because of possible damages to the ceramic due to the water hammer that occurs when the valve is forced suddenly to close. The requirements for HER and LER ceramic chambers are slightly different. Since the beam energy is higher in HER, more kicker magnets are needed, so it is necessary to shorten the overall length. On the other hand, the design beam current is bigger in LER, the power loss in LER ceramic chamber is 50% bigger than that of HER. The better cooling ability is required in LER ceramic chamber. Parameters of ceramic chamber used in SuperKEKB are summarized in Table 14.7. The ceramic chamber is racetrack shape in its inner side with diameter of 60mm and 40mm in horizontal and vertical respectively. Alumina ceramic was chosen as chamber material because of its mechanical strength and good metalizing characteristic for braze. The dimensional accuracy was required to the inner wall of ceramic. It was ground so that the flatness of inner wall surface is less than 0.1 mm in 10 mm square area. In order to match the level at the junction of ceramic and sleeve metal less than ± 0.2 mm difference, taper structure was chosen at the end. Figure 14.22(a) shows a simulation result of vertical magnetic field B_y as a function of longitudinal position Z where length of the ferrite core is assumed to be 350 mm. Figure 14.22(b) shows a ratio of effective magnetic field as a function of Z . Ceramic tube with a length of 500 mm covers 95% of the total field. The ceramic chamber was developed to be more compact than KEKB. The gap of horizontal kicker magnet was reduced from 90mm (KEKB) to 70mm (SuperKEKB). It

reduces the power of the power supply by 40%. Mo-Mn is a typical braze material to the ceramic. However it is weaker against water, because plated NI which is indispensable for Mn-Mo metallization, dissolves into water. In stead of Mn-Mo metallization, Ti with activated metallize method has been adopted. This technique has been chosen in KEKB, and no troubles has been seen during KEKB operation.



- : CT
- : Magnetic field with chamber
- : Magnetic field w/o chamber

Figure 14.23: Field penetration of the kicker magnet.

Penetration of the kicker magnetic field was investigated with the test bench. The rise time of horizontal the kicker magnetic field is measured by integrating a signal from a pickup coil inserted in the magnet gap. Figure 14.23 shows power supply output current as well as magnetic field with/without Ti-coated ceramic chamber. The thickness of Ti coating is set to $6 \mu m$. Observed rise time is less than 200 nsec that satisfy the requirement.

Ceramic chamber for HER Two types of ceramic chambers were developed for the HER beam abort system[15]. One is used for the vertical kicker magnet and the other is used for horizontal kicker magnets. The length of the vertical kicker chamber

Table 14.7: Parameters of ceramic chambers

	HER-H	HER-V	LER-H	LER-V	LER-Q
Power Loss/ceramic [kW]	1.8	1.8	2.7	2.7	2.7
Ti coating [μm]	5	5	6	6	6
Cu coating [μm]	100	100	All Cu	All Cu	All Cu
inner dimensions [mm]	60x40	60x40	60x40	60x40	60x40
Height/Width [mm]	67.5x87.5	67.5x87.5	88x68	88x68	88x68
Braze	Ag-Cu	Ag-Cu	Ag-Cu	Ag-Cu	Ag-Cu
Braze Metallization	Ti	Ti	Ti	Ti	Ti
Ceramic material	Alumina	Alumina	Alumina	Alumina	Alumina
No. of ceramic tubes	2x4	1	2x1	1	1x2
Ceramic length [mm]	500x8	500	500x2	500	500x2
Chamber Length [mm]	1128x4	580	1230	634	634x2
Structure	Straw	Straw	Double tube	Double tube	Double tube
Temperature rise [$^{\circ}C$]	8	8	14	14	14

is 580 mm. The chamber has 500 mm long ceramic tube with a thin Ti conduction layer deposited on the inner wall. The flange made of Cu has been chosen to minimize heating due to image beam current. The ceramic is connected to the Cu flange through a sleeve made of kovar. Kovar was chosen as metal brazes ring. It provides low thermal stress hermetic seal, because kovar has almost same coefficient of thermal expansion as alumina ceramic. And it also provides flexible transition between ceramic and massive flange. Kovar for vacuum seal and that of cooling water were brazed separately, because even one of them had damage, it won't give any damage to the other braze. The electron beam welding is used to connect Cu flange and kovar sleeve to avoid annealing of Cu flange. In order to suppress heating due to image current on the kovar, which has high permeability, copper electroforming is applied to deposit 100 μm thick Cu layer on the inner wall of Kovar sleeve.

The ceramic chamber for the horizontal kicker magnet comprises two pieces of ceramic tubes. Two ceramic tubes are combined with kovar sleeve, making a single chamber with 1128.3 mm. Each ceramic tube has cooling water path. The water flows into the ceramic tube at upper and lower inlet in one end and gets out from the other end. The ceramic chamber made from one piece of ceramic so that it has simple structure and relatively easy to assemble. Figure 14.24 shows copper electroforming inner wall of kovar sleeve and cut model of ceramic tube. The simple structure makes the ceramic chamber shorter.

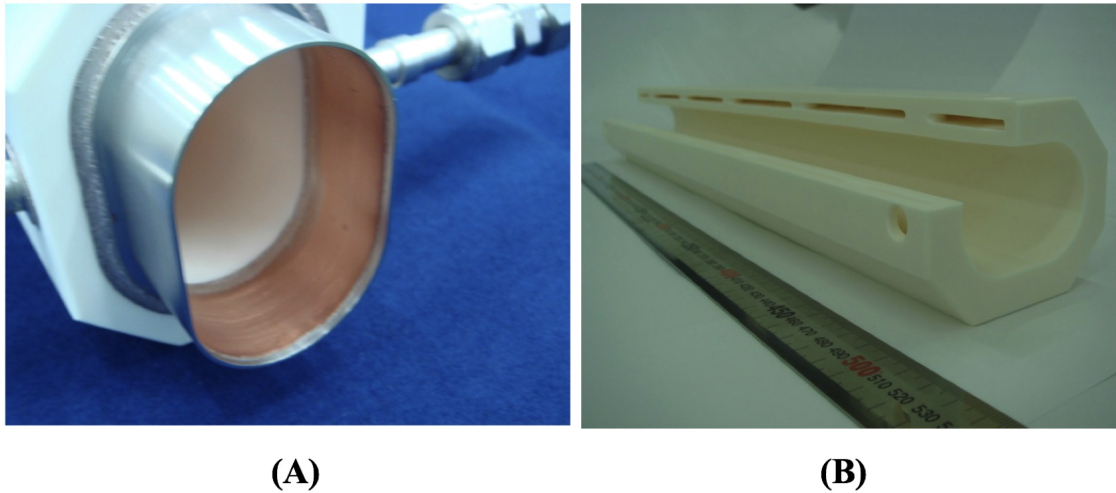


Figure 14.24: The ceramic chamber used in HER abort system. (A) shows kovar sleeve with $100\ \mu\text{m}$ thick Cu conducting layer at the inner wall. (B) is cut model of the ceramic tube which include cooling water path in the ceramic tube.

The Ti metallization of ceramic inner wall was produced by DC magnetron sputtering. Argon gas was chosen to make the plasma between the cathode of Ti rod and the anode which is a stainless-steel screen. Coating uniformity has been checked with thickness meter utilizing eddy-current. Target value of Ti coating thickness was set to $5\ \mu\text{m}$. Coating is relatively thick in the middle of ceramic tube and thin near the end. (Figure 14.25) When the target value is set to $5\ \mu\text{m}$, minimum $1\ \mu\text{m}$ Ti coating is guaranteed.

Ceramic chamber for LER In a similar way of HER, two types of ceramic chambers are developed. The pulsed quadrupole magnets and the vertical kicker use same type of ceramic chamber. The difference is only that the chamber of pulsed quadrupole magnet has a removal flange on one end. The length of ceramic chamber is 634 mm with 500 mm long ceramic tube having a thin Ti conduction layer deposited on the inner wall. Because the LER design current is larger than HER, the Cu sleeve, instead of kovar, has been adopted to connect to the Cu flange. Figure 14.26 shows Cu sleeve connected directly to the ceramic tube. Cu sleeve is connected to the Cu flange by the electron beam welding.

As same as HER, the ceramic chamber for horizontal kicker magnet is made of two ceramic tubes. They are combined via Cu sleeve, and total length of the chamber is 1230mm which is longer than HER. LER ceramic chamber has a double tube structure. Each ceramic tube is 5mm thick and secured adequate mechanical strength. Cooling

Typical Ti thickness for ceramic chamber

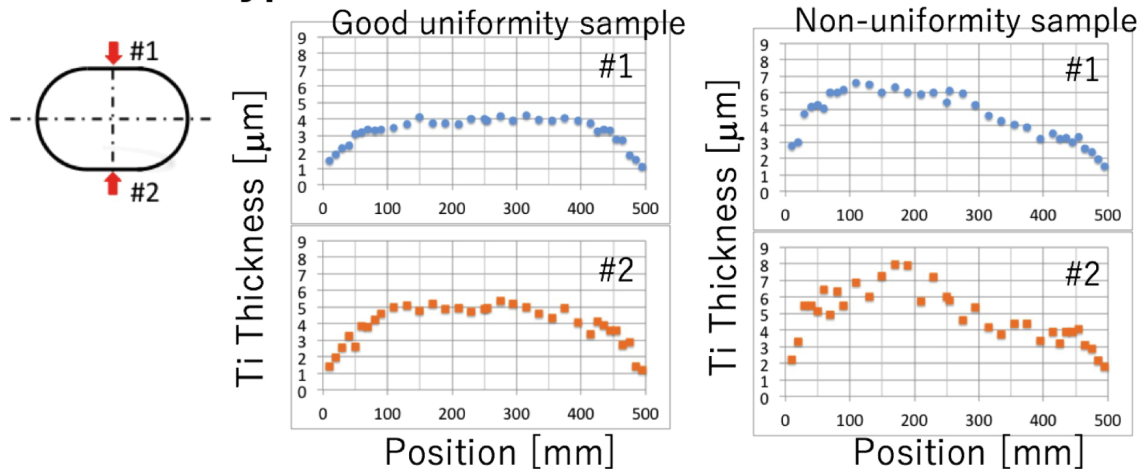


Figure 14.25: Ti coating thickness distribution in the inner wall of the ceramic along the beam direction.

water flows between inner and outer ceramic tubes. Since the total surface of the inner tube is cooled by water, it has a good cooling ability. As same as HER ceramic tube, the cooling water enters from the upper and lower tubes of one side and exits from the other side. Compared with HER ceramic chamber, the cooling ability is better, but the structure is complicated and total length became longer.

The extraction window and other vacuum chambers

The size of the abort window was designed so that the beam can pass through it safely full filling requirements of a 3.5σ beam size, an energy deviation of $\pm 1\%$, and a coherent oscillation simultaneously. The maximum vertical coherent oscillation is assumed to be about $50\sigma_y$ which is maximum acceptance limited by the vertical collimators to protect the Belle II detector. As for the horizontal coherent oscillation, we assume $5.6\sigma_x$ at maximum in the case of HER-BI and the beam abort is planed to be triggered when the oscillation amplitude exceeds this value. The designed cross section of the chambers for the HER and the LER are shown in Figure 14.27 and Figure 14.28, respectively. With the above considerations, the closest positions of the aborted beam to the inner surface of the chamber between the kickers and the Lambertson, are shown in Figure 14.27(a) and 14.28(a). The all chambers are designed to pass the aborted beam safely.

At the window, the aborted beam is confined within the region shown with the red rectangle in Figure 14.27(b) and 14.28(b). As shown in Figure 14.11(b) and 14.12(b), the horizontal orbit deviation of the aborted beam for the HER becomes maximum at

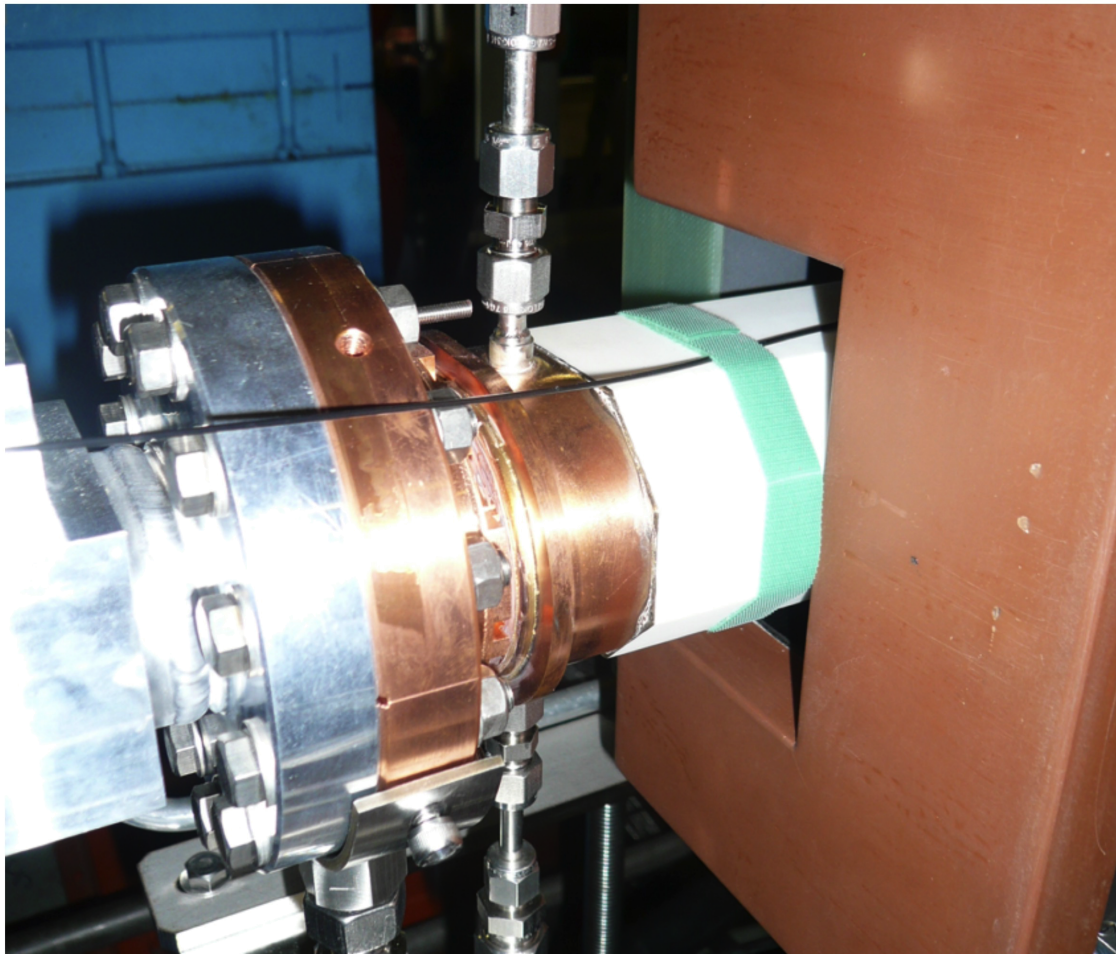


Figure 14.26: LER ceramic chamber with Cu sleeve connected directly to the ceramic tube.

the “Abort sextupole (1)” in the beam pipe. The horizontal and vertical sizes of this region are summarized in Table 14.8. Note that the vertical beam size of the aborted beam is larger than that of the stored beam due to the vertical dispersion created by the vertical kicker. We consider the tail of the aborted bunch train. The beam abort window was designed so as to include the red rectangle region. These beam pipes must have a larger aperture than the abort window.

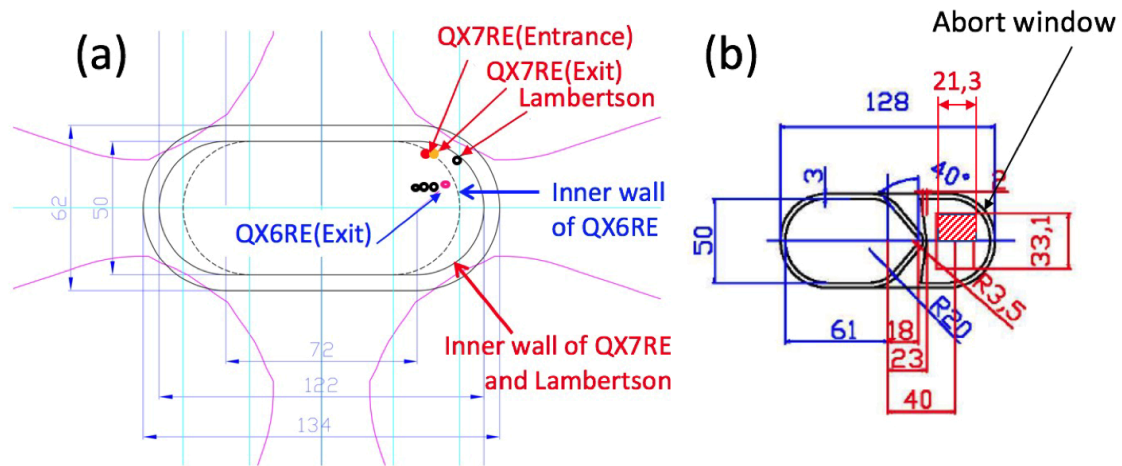


Figure 14.27: HER: (a) The cross section of the inner chamber of quadrupoles QX6RE and QX7RE which locate between the abort kickers and the entrance of Lambertson. The dots show the positions where the beam are closest to the chamber walls with the coherent oscillation. (b) The cross section of the abort window. The red rectangle shows the region where the aborted beam passes.

Table 14.8: The inner size of the Abort chamber which are installed in the Lambertson septum. The sizes full fills requirements of a 3.5σ beam size, an energy deviation of $\pm 1\%$, and a coherent oscillation simultaneously.

	HER (SI)	HER (BI)	LER (BI)
Horizontal size	$5.7\sigma_x$	$5.6\sigma_x$	$3.2\sigma_x$
Vertical size	$47\sigma_y$	$51\sigma_y$	$121\sigma_y$

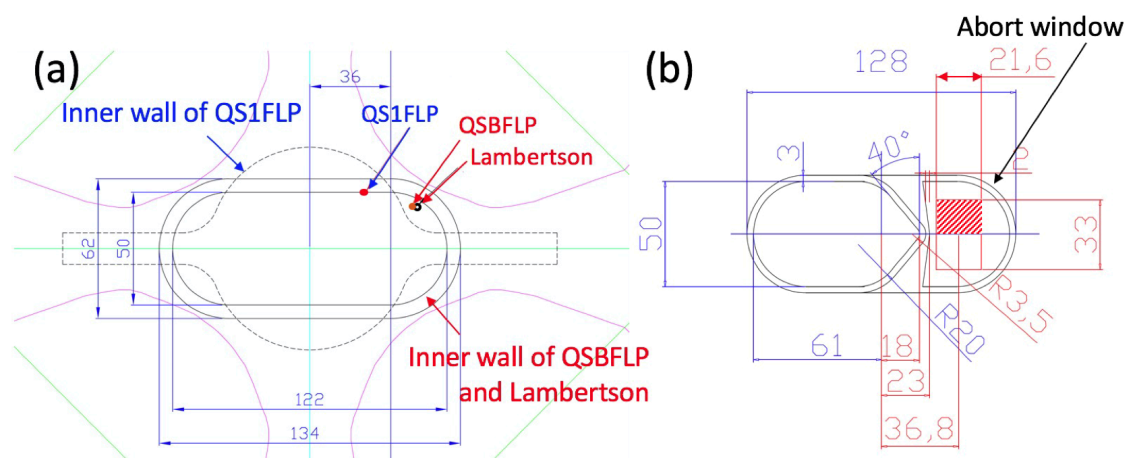


Figure 14.28: LER: (a) The cross section of the chambers for the inner chamber of quadrupoles QS1FLP (dotted line), and QSBFLP and the entrance of Lambertson (solid lines), which locate between the abort kickers and the Lambertson. The points show the positions where the beam are closest to the chamber walls with the coherent oscillation. (b) The cross section of the abort window. The red rectangle shows the region where the aborted beam occupies.

Bibliography

- [1] <http://www.aps.anl.gov/epics/>
- [2] J. Odagiri et al., “ The 9th Annual Meeting of Particle Accelerator Society of Japan ”, Aug. 8-11, 2012, pp. 206.
- [3] <https://github.com/ControlSystemStudio/cs-studio/wiki/BOY>
- [4] K. Yoshii et al., “ The 10th Annual Meeting of Particle Accelerator Society of Japan ”, Aug. 3-5, 2013
- [5] S.Sasaki *et al.*, "Upgrade of Abort Trigger System for SuperKEKB", ICALEPCE2015, MOPGF141
- [6] T.Naito *et al.*, "Performance of the timing system for KEKB", ICALEPCS'99, p214-p216
- [7] H.Ikeda *et al.*, "Beam Loss and Abort Diagnostics During SuperKEKB Phase-I Operation", IBIC2016, TUAL03
- [8] H.Ikeda *et al.*, "Beam Loss Monitor at SuperKEKB", IBIC2014, TUPD22
- [9] T. Mimashi *et al.*, "SuperKEKB Beam Abort System", IPAC2014, MOPRO023
- [10] T. Mimashi *et al.*, "The Beam Test for the Ti Extraction Window Damage", IPAC2014, MOPRO024
- [11] T. Mori *et al.*, "Design Study of Beam Injection for SuperKEKB Main Ring", IPAC2014, TUPPR089
- [12] N. Iida *et al.*, "Optics Design and Observation for the Beam Abort System in The SuperKEKB HER", IPAC2017, WEPIK007
- [13] Japan Isotope Association, "Isotope Handbook 3rd Edition", 1995, p426

- [14] N. Iida *et al.*, "A Position Monitor for the Aborted Beam in KEKB", EPAC2008, WEPP061
- [15] T. Mimashi *et al.*, "Ceramic Chamber Used in SuperKEKB High Energy Ring Beam Abort System", IPAC2017, MEPIK011
- [16] M.Kikuchi, private communication, unpublished.